Recursive Selective Harmonic Elimination for Multilevel Inverters: Mathematical Formulation and Experimental Validation

C. Buccella, M.G. Cimoroni, C. Cecati
University of L'Aquila & DigiPower srl
67100 L'Aquila, Italy

A.O. Di Tommaso, R. Miceli, C. Nevoloso, G. Schettino
University of Palermo
90128 Palermo, Italy

***Abstract*—A recursive method that eliminates $n+1$ harmonics and their respective multiples from the output voltage of a cascaded H-bridge multilevel inverters with $s = 2^n$ dc sources $(n = 1,\ 2,\ 3,\ ...)$ is proposed. It solves 2×2 linear systems with not singular matrices and always gives an exact solution with very low computational effort. Simulated results in three-phase five, nine, seventeen and thirty three level CHB inverters, and experimental results in five-level inverter demonstrate the validity of the method.**

***Index Terms*—Multilevel Inverter, Modulation, Selective Harmonics Elimination, Total Harmonic Distortion (THD), Efficiency.**

Nomenclature

l	number of levels
s	number of DC voltage sources
k	harmonic order
m	modulation index
n	integer number such that $s = 2^n$
v_{out}	output voltage of the multilevel inverter [V]
V	DC voltage feeding each H-bridge [V]
V_{dc}	rated voltage [V]
V^*	DC voltage feeding each H-bridge [p.u.]
$\frac{4V^*}{k\pi}H_k$	k^{th} harmonic amplitude
α_i, $i = 1, \ldots, s$	switching angles [rad]
$\alpha_i^{(p)}$, $i = 1, \ldots, s,\ p = n, \ldots, 1$	intermediate variables (for $p = 1$, $\alpha_i^{(1)} = \alpha_i$)
$\frac{4V^*}{k\pi}H_k^{(p)}$	intermediate variables (for $p = 1$, $\frac{4V^*}{k\pi}H_k^{(1)} = \frac{4V^*}{k\pi}H_k$).

I. Introduction

Due to their capability to produce approximated sinusoidal output voltages, multilevel inverters are gaining applications in many fields including renewable energy systems, electric traction, industry, smart grids[1]-[3]. The shape of their waveforms gives significant improvements over conventional two-level converters, in terms of lower total harmonics distortion (THD), higher efficiency, increased voltage/power handling capability and reduced component stress, hence higher reliability. The main responsible for such features is the adopted modulation technique, which is highly influential both in terms of performance and implementation complexity. Basically, a modulation technique consists on the determination of a set of switching angles, which, then, can be regarded as the unknowns of the modulation problem. Usually, modulation algorithms are classified in three distinct categories: selective harmonic elimination (SHE), selective harmonic mitigation (SHM) and pulse width modulation (PWM) algorithms. In general, the first two approaches operate at fundamental frequency, the latter at high frequency, but, usually, at values significantly lower than in conventional two level PWM inverters [4]-[10]. Since the lower the frequency, the higher the overall efficiency, when possible, i.e. in low dynamic systems, it is desirable to adopt SHE or SHM, while multilevel PWM is usually adopted in those applications requiring high bandwidth control. Among the numerous papers on the topic, Sajadi *et al*. [11] proposed a SHE technique for high-power asymmetrical CHB inverters employed for static VAR compensation (STATCOM) application, which is capable to eliminate low-order harmonics, to reduce converter losses and to regulate the voltage of each dc-link capacitor. To further improve the quality of the output voltages, Buccella *et al*. proposed to vary the amplitudes of the dc sources, introducing the pulse amplitude width modulation (PAWM) [10], that increases the number of deleted harmonics at fundamental switching frequency. Law Kah Haw *et al*. [12] proposed a low-switching frequency multilevel SHE-PWM technique for CHB inverters used in transformerless STATCOM systems, that provides constant switching angles and linear pattern DC voltage levels over the full range of the modulation index by employing DC/DC buck converters which operate at a relatively low switching frequency of 2 kHz. Padmanaban *et al*. in [13] proposed a SHE technique for PV systems equipped with a CHB multilevel inverter and boost DC/DC converters, based on an integrated artificial neural network and a Newton Raphson (NR) numerical approach. As discussed in the review paper [14], SHE and SHM modulation techniques are widely used in large electrical drives for traction applications. For instance, Zhituo Ni *et al*. [15] proposed a fault-tolerant seven-level CHB motor drive with a non-symmetrical SHE algorithm that provides a better voltage profile and higher output line voltage amplitude with respect to a conventional frequency phase-shifted compensation approach (FPSC); Steczek *et al*. proposed to combine SHE and SHM-PWM for railway applications [16]; Schettino *et al*. used an innovative SHM algorithm in an interior permanent magnet synchronous (IPMSM) drive, obtaining better current THD and drive efficiency than with a conventional multi-carrier PWM technique [17].

This article has been accepted for publication in IEEE Journal of Emerging and Selected Topics in Power Electronics. This is the author's version which has not been fully edited and content may change prior to final publication. Citation information: DOI 10.1109/JESTPE.2022.3221154

This paper deals with selective harmonics elimination at fundamental frequency. In this framework, it is necessary to identify and implement a method capable to find the solutions of the SHE equations or of a non-linear equations system, corresponding to converter switching angles. At this regard, numerous techniques have been proposed, including iterative approaches [18], optimization methods [19]-[20] and mathematical solutions [21]-[22]. The first topology presents set of angles that depends on the initial values, which initially are unknowns and the solution could be divergent. The second topology includes genetic algorithms (GAs), bee algorithms (BAs) and in general artificial intelligence-based algorithms (AGAs) that are not significantly affected by initial values but are complex to implement and present high computational costs [23]-[25]. The third typology solves the transcendental equations by algebraic algorithms that are generally computationally efficient. In general, the main drawback is related to the difficulty of solving in real-time the transcendental equations but accurate harmonics cancellation is guaranteed [26]-[27]. For instance, [28] proposed an offline computing stage in which the nonlinear equations are linearized by using the theories of symmetric polynomials and Gröbner, then, the linear equations are solved online and their solutions are used to construct a polynomial whose real roots are the switching angles. For CHB 5-level inverters, SHE analytical solutions can be obtained in real time as described in [7], [8]. Such a method can be extended to a higher number of levels and ensures the elimination of n harmonics.

This work aims to propose a new SHE method at fundamental switching frequency for CHB multilevel inverters which allows the elimination of more harmonics with respect to the traditional SHE methods. In particular, it allows the elimination of $n+1$ harmonics and their multiples from the output voltage waveform of an l-level CHB inverter with s equal DC sources V depending on modulation index m. The number of voltage levels has to be $l = 2s+1$, with $s = 2^n$ and $n = 1,\ 2,\ 3,\ \ldots$. The innovation of this procedure is the recursive application of the Prosthaphaeresis formulas that allow obtaining the s switching angles by solving $s-1$ 2×2 linear system. The modulation index is directly correlated with the amplitude of the DC sources through a proportional coefficient that depends on the eliminated harmonics. In this way, the converter performance in terms of voltage distortion and converter efficiency does not depend on the modulation index.

The main advantages of the proposed procedure are summarized in the following:

- in inverters with a low number of levels, it returns a higher number of deleted harmonics and a lower THD than the classical SHE technique described in [8];
- it always returns an analytically exact solution. It is worth to notice that, by using the method proposed in [8], it is not possible to find a solution for all modulation index values and in some cases there are multiple solutions;
- being analytical, computational demand is very low, therefore, it could be easily implemented in real-time at low cost [29];

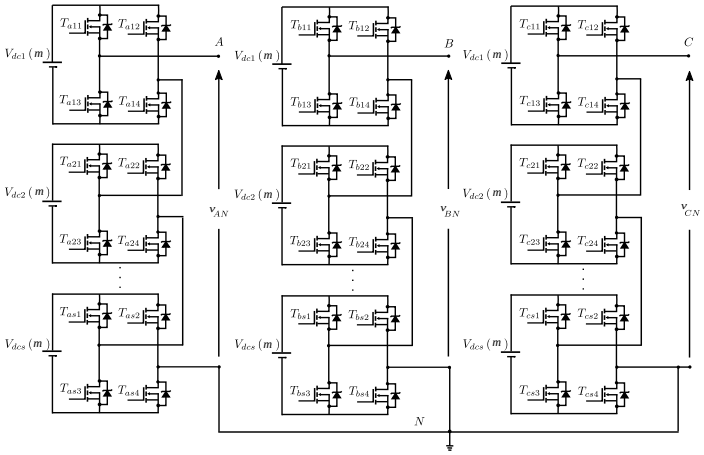

Fig. 1. Three-phase l-level CHB inverter.

- the modulation index can be changed in a continuous range from zero to its maximum value;
- switching angles and THD do not depend on the modulation index m;
- the modulation index linearly depends on the DC voltage amplitudes.

The paper is structured as follows: Section II presents the mathematical model of three-phase l-level CHB inverter. Section III describes the proposed method for the elimination of $n+1$ harmonics. Section IV presents the implementation. Section V discusses the computational complexity of the proposed SHE approach. Section VI presents the simulation results obtained with several distinct CHB inverter configurations. Section VII presents the experimental analysis that validates the effectiveness of the proposed method. Section VIII provides a comparison between the proposed SHE approach and other recent methods present in the literature. Finally, Section IX summarizes the key features of the proposed SHE method and reports the study conclusions.

II. Mathematical model

Figure 1 shows a three-phase, l-level, CHB inverter. The following constraint is imposed to the number of levels: $l = 2s+1$, where $s = 2^n$ is number of DC sources for each phase, being $n = 1,\ 2,\ 3,\ ...$ integer number. Due to previous assumption, the proposed procedure can be only used with five, nine, seventeen, thirty-three, sixty-five or more levels inverters.

The H-bridges are feed by equal DC sources, which amplitudes depend on the modulation index m, i.e.:

$$V_{dc1}(m) = V_{dc2}(m) = \cdots = V_{dcs}(m) = V(m) \tag{1}$$

whose values in per unit (p.u.) are:

$$V^* = \frac{V}{V_{dc}} = C \cdot m \tag{2}$$

where V_{dc} is the rated voltage, C is a positive coefficient and m is equal to:

$$m = \frac{\pi \widetilde{H}_1}{4s} \tag{3}$$

being $\widetilde{H}_1$ the amplitude of the fundamental harmonic in p.u. . Considering the phase A, the Fourier series of the line-to-neutral output voltage v_{AN} is:

$$v_{AN}(\omega t) = \frac{4}{\pi} \sum_{k=1,\,3,\,5,\,\ldots}^{\infty} \frac{1}{k} V(m) H_k \sin(k\omega t) \tag{4}$$

where:

$$H_k = \sum_{i=1}^{s} \cos(k\alpha_i), \tag{5}$$

being α_i the switching angles with:

$$0 < \alpha_i < \frac{\pi}{2}, \quad i = 1,\, 2,\, 3,\, \ldots s \tag{6}$$

and $\widetilde{H}_k$ the amplitude of the k-order harmonic, expressed as:

$$\widetilde{H}_k = \frac{4}{\pi} \frac{V^*}{k} H_k. \tag{7}$$

From (2) follows that:

$$C = \frac{s}{\sum_{i=1}^{s} \cos(\alpha_i)}. \tag{8}$$

III. Proposed method

With the previous assumptions, the following mathematical system can be defined to eliminate the $n+1$ harmonics of order $r_1, r_2, \ldots, r_{n+1}$ from the phase voltage of the three-phase l-level CHB inverter:

$$\begin{cases} H_{r_1}(\cos(r_1\alpha_1), \ldots, \cos(r_1\alpha_s)) = 0 \\ \vdots \\ H_{r_j}(\cos(r_j\alpha_1), \ldots, \cos(r_j\alpha_s)) = 0 \\ \vdots \\ H_{r_{n+1}}(\cos(r_{n+1}\alpha_1), \ldots, \cos(r_{n+1}\alpha_s)) = 0. \end{cases} \tag{9}$$

In order to calculate the unknowns α_i $i = 1, 2, ..., s$ and to solve (9), a recursive procedure can be implemented as described in the following steps.

Step 1. Calling $H_k^{(1)} = H_k$ and $\alpha_i^{(1)} = \alpha_i$, being $i = 1, 2, ..., s$, for k that can assume the values $r_1, r_2, \cdots, r_{n+1}$, applying Prosthaphaeresis formulas, it follows that:

$$\begin{aligned} H_k^{(1)} &= \sum_{i=1}^{s} \cos\left(k\alpha_i^{(1)}\right) = \sum_{i=1}^{s/2} \left[\cos\left(k\alpha_{2i-1}^{(1)}\right) + \cos\left(k\alpha_{2i}^{(1)}\right)\right] \\ &= 2 \sum_{i=1}^{s/2} \cos\left(k\frac{\alpha_{2i-1}^{(1)} + \alpha_{2i}^{(1)}}{2}\right) \cos\left(k\frac{\alpha_{2i-1}^{(1)} - \alpha_{2i}^{(1)}}{2}\right). \end{aligned} \tag{10}$$

By (10), the equation $H_{r_1}^{(1)} = 0$ can be satisfied when:

$$\frac{\alpha_{2i-1}^{(1)} + \alpha_{2i}^{(1)}}{2} = \frac{\pi}{2r_1} \quad i = 1, ..., \frac{s}{2}. \tag{11}$$

By introducing the new variables $\alpha_i^{(2)} = \frac{\alpha_{2i-1}^{(1)} - \alpha_{2i}^{(1)}}{2}$, $i = 1, \ldots, \frac{s}{2}$, the following relations are obtained:

$$\begin{cases} \alpha_{2i-1}^{(1)} + \alpha_{2i}^{(1)} = \frac{\pi}{r_1} \\ \alpha_{2i-1}^{(1)} - \alpha_{2i}^{(1)} = 2\alpha_i^{(2)} \end{cases}, \; i = 1, \ldots, \frac{s}{2}. \tag{12}$$

Substituting (12) in (10), the following expression $H_k^{(1)}$ is obtained:

$$H_k^{(1)} = 2\cos\left(k\frac{\pi}{2r_1}\right) H_k^{(2)} \tag{13}$$

where:

$$H_k^{(2)} = \sum_{i=1}^{s/2} \cos\left(k\alpha_i^{(2)}\right). \tag{14}$$

It is clear that $H_k^{(1)} = 0$ for each $k = jr_1$, with $j = 1, 3, 5, ...$, i.e. for all odd multiples of r_1.

Steps from 2 to n. By imposing $H_{r_q}^{(q)} = 0$, $q = 2, \ldots n$, by applying again Prosthaphaeresis formulas and by introducing the new variables $\alpha_i^{(q+1)} = \frac{\alpha_{2i-1}^{(q)} - \alpha_{2i}^{(q)}}{2}$, $i = 1, \ldots, \frac{s}{2^q}$, the following non singular systems are obtained:

$$\begin{cases} \alpha_{2i-1}^{(q)} + \alpha_{2i}^{(q)} = \frac{\pi}{r_q} \\ \alpha_{2i-1}^{(q)} - \alpha_{2i}^{(q)} = 2\alpha_i^{(q+1)} \end{cases}, \; i = 1, \ldots, \frac{s}{2^q} \tag{15}$$

and

$$H_k^{(q)} = 2\cos\left(k\frac{\pi}{2r_q}\right) H_k^{(q+1)}, \; q = 2, \ldots n \tag{16}$$

where:

$$H_k^{(q+1)} = \sum_{i=1}^{s/2^q} \cos\left(k\alpha_i^{(q+1)}\right). \tag{17}$$

Also in these cases, $H_k^{(q)} = 0$ for each $k = jr_q$, $j = 1, 3, 5, ...$, i.e. for all odd multiples of r_q.

Step n+1. As the last step, by (17), $H_k^{(n+1)} = \cos\left(k\frac{\alpha_1^{(n)} - \alpha_2^{(n)}}{2}\right)$ and imposing $H_{r_{n+1}}^{(n+1)} = 0$ the (15), for $q = n$ becomes:

$$\begin{cases} \alpha_1^{(n)} + \alpha_2^{(n)} = \frac{\pi}{r_n} \\ \alpha_1^{(n)} - \alpha_2^{(n)} = \frac{\pi}{r_{n+1}} \end{cases} \tag{18}$$

therefore, by (13) and (16) follows that:

$$H_k^{(1)} = 2^q \prod_{j=1}^{q} \cos\left(k\frac{\pi}{2r_j}\right) H_k^{(q+1)}, \; q = 1, \ldots n \tag{19}$$

and for $q = n$, by (18) $H_k^{(n+1)} = \cos\left(k\frac{\pi}{2r_{n+1}}\right)$ and by (19) follows that:

$$H_k^{(1)} = 2^n \prod_{j=1}^{n+1} \cos\left(k\frac{\pi}{2r_j}\right). \tag{20}$$

The unknown switching angles $\alpha_i^{(1)} = \alpha_i$ in (12) are computed after solving (18), (15) for $q = 2, \ldots, n-1$ and (12).

IV. Implementation

Proposed recursive method consists of the algorithm shown in the flowchart of Fig. 2. It starts from the solution of (18) and stops with the solutions of the $s/2 - \text{th}$ systems in (12).

The algorithm considers the matrix:

$$A = \begin{pmatrix} 1 & 1 \\ 1 & -1 \end{pmatrix} \tag{21}$$

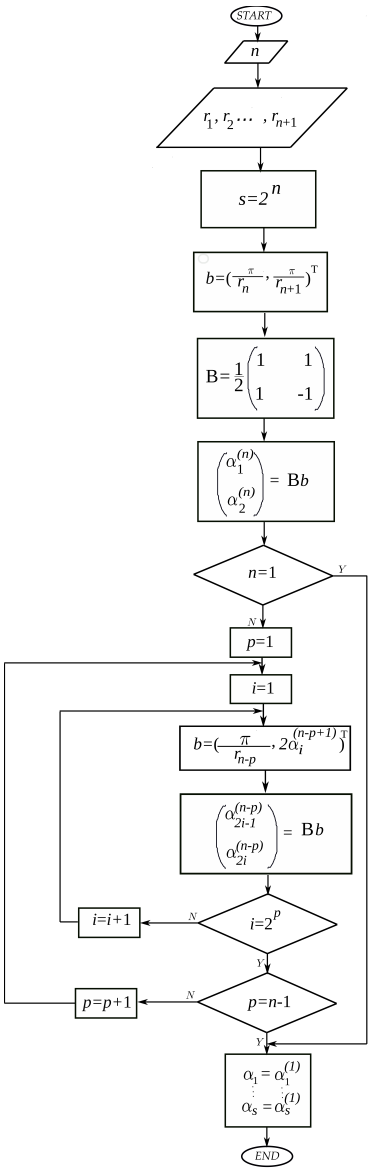

Fig. 2. Flowchart of switching angles computation algorithm.

its inverse $\boldsymbol{B} = \frac{1}{2}\boldsymbol{A}$ and $r_1, \ldots, r_{n+1}$ with $n \geq 1$ such that $s = 2^n$ and obtains the solution as:

$$\begin{pmatrix} \alpha_1^{(n)} \\ \alpha_2^{(n)} \end{pmatrix} = \boldsymbol{B} \begin{pmatrix} \frac{\pi}{r_n} \\ \frac{\pi}{r_{n+1}} \end{pmatrix}. \tag{22}$$

If $n > 1$, for $p = 1,\ ...,\ n-1$, 2^p systems are solved as:

$$\begin{pmatrix} \alpha_{2i-1}^{(n-p)} \\ \alpha_{2i}^{(n-p)} \end{pmatrix} = B \begin{pmatrix} \frac{\pi}{r_{n-p}} \\ 2\alpha_i^{(n-p+1)} \end{pmatrix}, \quad i = 1, ..., 2^p \tag{23}$$

The switching angles (6) are $\alpha_i^{(1)}$ $i = 1, 2 \cdots, s$ and they are obtained by solving (23) when $p = n - 1$.

V. Computational complexity

In the flowchart in Fig. 2, it is possible to observe that a 2×2 linear system has been solved before entering in the double cycle in p and i. Inside the inner cycle, in the variable i, 2^p linear systems with p in the range $[1,\ n-1]$ are solved, therefore, the number of solved systems is:

$$N_s = 1 + \sum_{p=1}^{n-1} 2^p = \sum_{p=0}^{n-1} 2^p = \frac{2^n - 1}{2 - 1} = 2^n - 1 = s - 1. \tag{24}$$

The computational complexity T_a of the proposed algorithm is:

$$T_a = (s-1)\, T_{\mathrm{sc}} \tag{25}$$

where T_{sc} is a matrix-vector scalar product with a 2×2 matrix, that is $T_{sc} = 2T_{\mathrm{addition}} + 4T_{\mathrm{multiplication}}$ where T_{addition} and $T_{\mathrm{multiplication}}$ are time factors for addition and multiplication operations, respectively.

A. Application of the method to a three-phase 5-level inverter

Using a 5-level CHB inverter, proposed method can eliminate two harmonics. This case is particularly simple and its implementation requires very limited effort. In fact, the method is not recursive and the switching angles are computed as follows:

$$\begin{cases} \alpha_1 = \frac{\pi}{2}\left(\frac{1}{r_1} + \frac{1}{r_2}\right) \\ \alpha_2 = \frac{\pi}{2}\left(\frac{1}{r_1} - \frac{1}{r_2}\right) \end{cases} \tag{26}$$

therefore $T_a = 2T_{\mathrm{addition}} + 2T_{\mathrm{multiplication}}$.

B. Comparison with the SHE algorithm [8]

In [8], the analytical solution, i.e. the values of the switching angles, has been found for a 5-level CHB inverter, operating at fundamental frequency, considering equal and fixed source voltages that do not depend on the modulation index. For a fixed modulation index m, the computational complexity of the modulation algorithm in [8] is:

$$T_{a[8]} = (T_{\cos} + T_{\arccos} + 3T_{\mathrm{multiplication}} + 2T_{\mathrm{division}}) \tag{27}$$

where $T_{\cos}$ and $T_{\arccos}$ are time factors of cos function and arccos functions, respectively. Therefore, being $s = 2$, $T_a = T_{\mathrm{sc}} < T_{a[8]}$.

Other methods described in literature are iterative, therefore, they present poorly predictable and, in general, high computational complexity [4], [30].

VI. Simulated results

In order to validate the effectiveness of the proposed approach, numerical analysis has been carried out using Matlab®. Figure 3 and 4 show the phase voltage harmonic analysis and the corresponding THD for a three-phase, nine, seventeen, and thirty-three -level CHB inverter, which can be considered cases of practical interest.

This article has been accepted for publication in IEEE Journal of Emerging and Selected Topics in Power Electronics. This is the author's version which has not been fully edited and content may change prior to final publication. Citation information: DOI 10.1109/JESTPE.2022.3221154

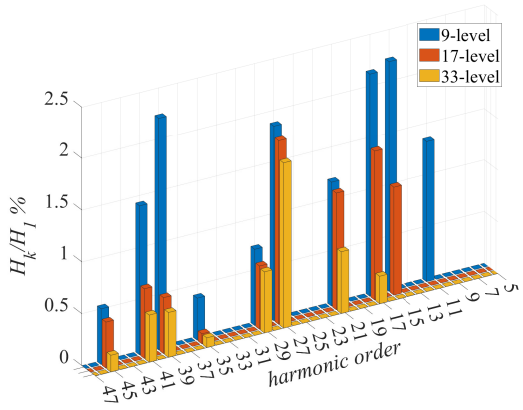

Fig. 3. Comparative phase voltage harmonic analysis.

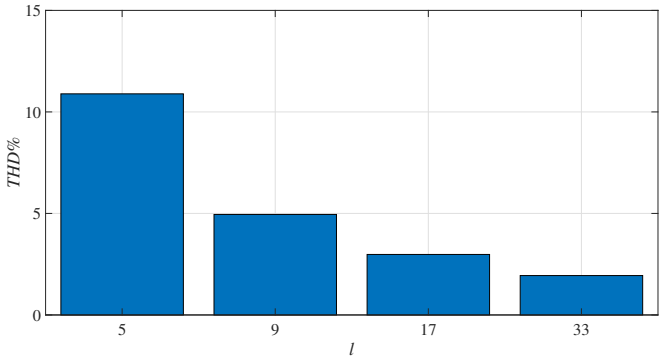

Fig. 4. Phase voltage THD% vs CHB inverter level number (l).

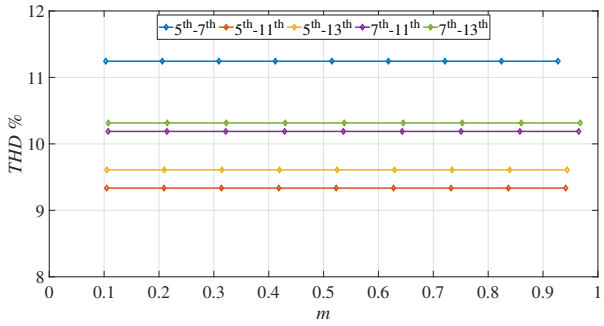

(a) THD % vs. modulation index

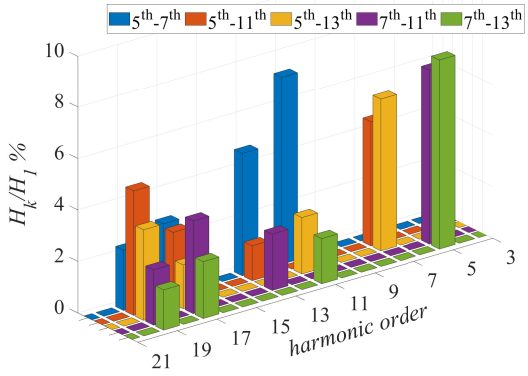

(b) Harmonics spectra comparison

Fig. 5. Simulation analysis of three-phase five-level CHB inverter.

The impact of missing harmonics on the THD can be various, therefore, it is interesting to consider and compare several combinations of eliminated harmonics. Since the prototype available in the Sustainable Development and Energy Saving Laboratory (SDESLAB) of the University of Palermo is a three-phase five-level CHB inverter, this detailed analysis has been restricted to this CHB topology for consequent experimental validation. Five cases have been considered as reported in Table I. Control angles have been evaluated for each case study and the corresponding modulation index range, expressed in (28) by considering (3) and (5), is reported below:

$$m = \frac{V}{V_{DC}} \cdot [\cos\alpha_1 + \cos\alpha_2]\,. \tag{28}$$

It must be noted that the expression (28) describes the relation of m interval with the constraint regarding the number of the DC sources and control angles, and consequently with the $n+1$ eliminated harmonics. Therefore, by fixing n, the value of the modulation index depends only on the DC voltage amplitude. Fig. 5 shows the THD% trend vs. modulation index (Fig. 5a) and the low order harmonics spectra comparison (Fig. 5b) for each case study. In Case 1, the lowest values of THD% have been obtained by eliminating both the 5^{th} and the 11^{th} harmonic, moreover, it can be observed that the THD% values do not depend on the modulation index. In Case 2, by eliminating the 5^{th} and 11^{th} harmonics (orange bar graph), the predominant harmonics are 7^{th} and 19^{th} with an amplitude of about 4%, as shown in Fig. 5b, where low order harmonics spectra are compared. Thus, this result explains the lower values of the THD% in this case.

VII. Experimental Results

A test rig, shown in Fig. 6, has been assembled at SDESLab. It is composed by:

- a three-phase five-level CHB MOSFET-based inverter obtained assembling six distinct H-bridges controlled by a control board employing an Intel-Altera Cyclone III FPGA, programmed in VHDL with 32-bit arithmetics. The system is produced by DigiPower and the main technical data are reported in Table II. The power rating of each H-Bridge module is 5 kW, obtaining a 30 kW power rating for a three-phase five-level CHB inverter prototype;
- six programmable DC power supplies RSP-2400 whose main technical data are reported in Table III ([31]);
- a passive electric load $R-L$ (constantan rheostats with $R = 20\ \Omega$ and $L = 10$ mH);
- a Teledyne LeCroy WaveRunner Oscilloscope 640Zi, two Yokogawa 700924 differential voltage probes and two Yokogawa 701933 current probes;
- two Yokogawa power meters (WT 330 and WT 130).

Fig. 7 shows a schematic representation of the implemented system, including measurement circuit. The experimental validation was carried out in two steps and the experimental

results were compared with those obtained with the SHE algorithm [8]. In the first analysis, load tests with a $R-L$ load ($R = 20\ \Omega$ and $L = 10$ mH) were carried out to validate the proposed approach and the line voltage harmonic content of the proposed algorithm was reported by using the THD% as a comparative parameter at no-load working conditions. After that, the converter efficiency were measured in the cases summarized in Table I and compared with those measured implementing the SHE algorithm discussed in [8].

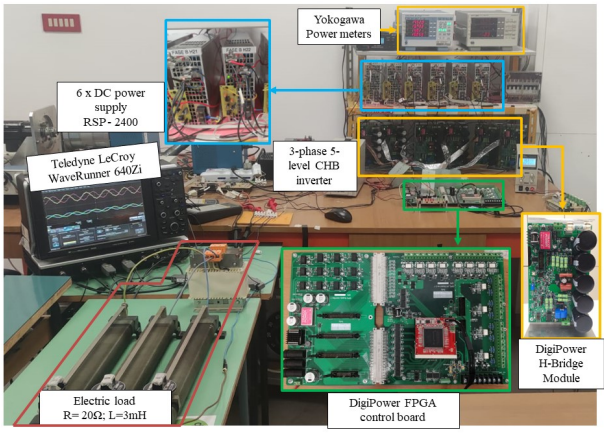

Fig. 6. Test bench.

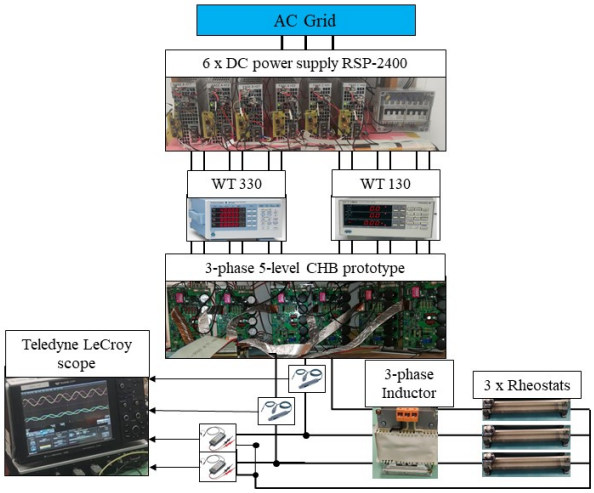

Fig. 7. Schematic representation of the circuit with measurement points.

A. Validation and converter THD analysis

In order to demonstrate the effectiveness of the proposed approach, Fig. 8 shows the line voltage (yellow curve), phase current (cyan curve) and corresponding voltage harmonic distribution in the frequency domain (red bar graph) for each analyzed case at DC input voltages equal to 40 V. The voltage, current and time scales were set to 50 V/div, 2 A/div and 5 ms/div, respectively; the harmonic spectra in the frequency domain presents a voltage scale equal to 20 V/div and a frequency scale equal to 200 Hz/div. As shown in Fig.8, it should be noted that the selected harmonics were eliminated in each case demonstrating the effectiveness of the proposed algorithm. In order to evaluate dynamic performances during the elimination of pairs of harmonics described in Table I, several tests were carried out for DC voltage steps, corresponding to the modulation index step inside the interval shown in Table I. In this analysis, it is necessary to highlight that the switching angles are constant within all modulation index range, resulting in a negligible impact on CHB inverter dynamic performances. Therefore, the CHB inverter transient behaviour depends only on the time variation of DC voltage power supplies.

TABLE I
CASE STUDIES OF THE PROPOSED ALGORITHMS

Case	Eliminated harmonics	Control angles [rad]	Modulation index
1	5^{th} and 7^{th}	$\alpha_1 = 0.5386$ $\alpha_2 = 0.0898$	$0 \leq m \leq 0.9272$
2	5^{th} and 11^{th}	$\alpha_1 = 0.4570$ $\alpha_2 = 0.1714$	$0 \leq m \leq 0.9414$
3	5^{th} and 13^{th}	$\alpha_1 = 0.4350$ $\alpha_2 = 0.1933$	$0 \leq m \leq 0.9441$
4	7^{th} and 11^{th}	$\alpha_1 = 0.3672$ $\alpha_2 = 0.0816$	$0 \leq m \leq 0.9650$
5	7^{th} and 13^{th}	$\alpha_1 = 0.3452$ $\alpha_2 = 0.1036$	$0 \leq m \leq 0.9678$

TABLE II
MAIN PARAMETERS OF THE DIGIPOWER CHB INVERTER EMPLOYING MOSFET IRFB4115PBF.

Quantity	Symbol	Value
Voltage	V_{dss}	150 V
Resistance	R_{DSon}	$9.3\,m\Omega$
Current	I_D	104 A
Turn on delay	T_{Don}	18 ns
Rise time	T_R	73 ns
Turn off delay	T_{Doff}	41 ns
Fall time	T_F	39 ns
Reversal recovery	T_{RR}	86 ns

TABLE III
MAIN DATA OF DC POWER SUPPLY RSP-2400.

Section	Quantity	Value
Output	DC Voltage	48 V
	Rated Current	50 A
	Rated Power	2400 W
	Voltage rise time	80 ms (Max) at full load
Input	Voltage range AC	$180 - 264$ V
	Frequency range	$47 - 63$ Hz
	Efficiency	91.5%
	AC current	12 A/230 VAC

This article has been accepted for publication in IEEE Journal of Emerging and Selected Topics in Power Electronics. This is the author's version which has not been fully edited and content may change prior to final publication. Citation information: DOI 10.1109/JESTPE.2022.3221154

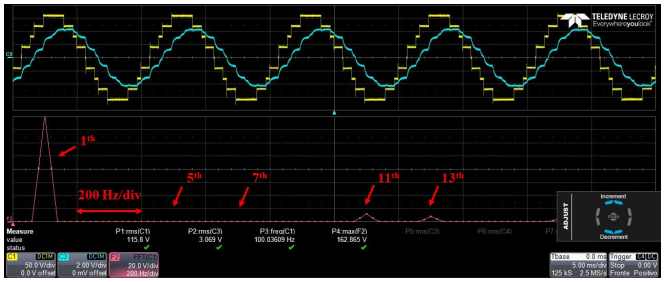

(a) SHE 5th and 7th – V= 40 V.

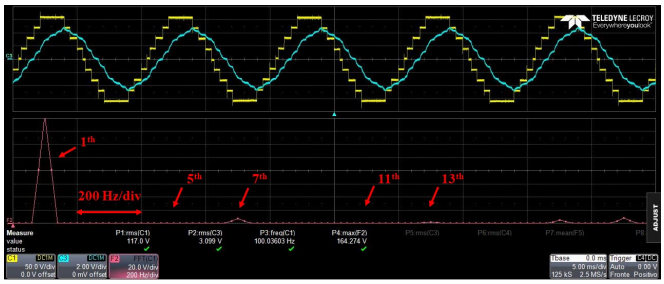

(b) SHE 5th and 11th – V= 40 V.

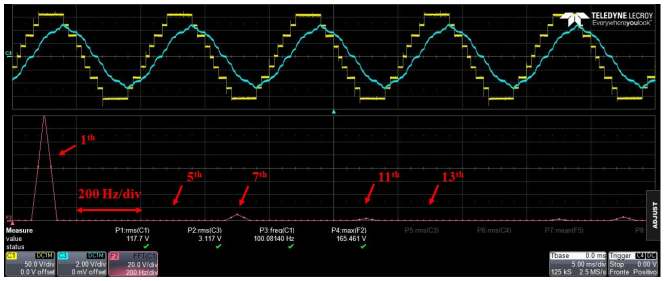

(c) SHE 5th and 13th – V= 40 V.

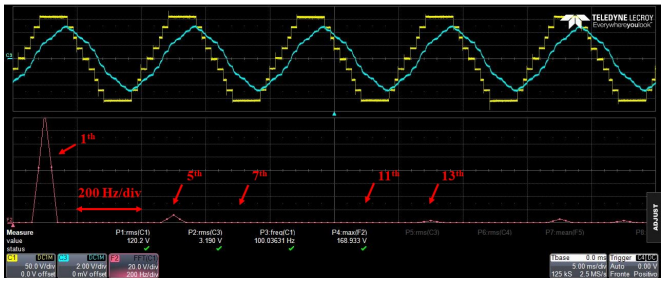

(d) SHE 7th and 11th – V= 40 V.

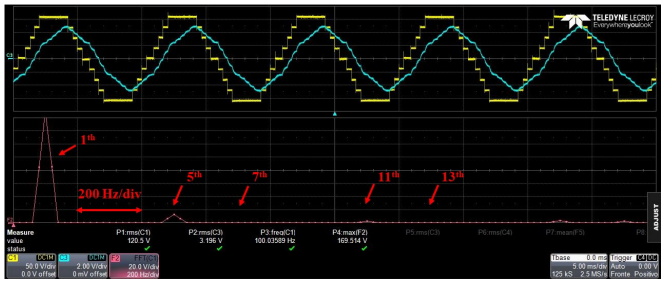

(e) SHE 7th and 13th – V= 40 V.

Fig. 8. CHB inverter experimental results: line voltage (yellow curve) , phase current (cyan curve) and voltage harmonic spectra (red bar graph).

In order to show the benefit described impact on CHB inverter dynamic performances, the high-side gate signals of each H-bridge module of the same phase, input DC voltages of the same phase, load phase voltage and phase current were acquired and analyzed. By way of example, Fig. 9 shows high-side gate signals of H-bridge modules (white, purple, orange and red curves), the load phase voltage (cyan curve), phase current (green curve) and relative input DC voltages (yellow and violet curves) of the CHB inverter when DC voltage input values change from 20 V to 40 V. The corresponding modulation index values were calculated by (28). In detail, Fig. 9a and Fig. 9b show the CHB inverter transient behaviour with the proposed approach by eliminating of 5th and 13th harmonics under modulation index variation from m=0.34 to m=0.69 and eliminating the 7th and the 13th harmonic under modulation index variation from m=0.35 to m=0.7, respectively. It can be noticed that the transient behaviour expires after about 50 ms, where the high-side gate signals are not affected by transients, by confirming the negligible impact of the algorithm computation on system dynamic performances. Similar results were obtained for all analyzed cases. The detected DC voltage time transient is attributable to the time constant of the DC power supply only, that is comparable with the rise time reported in power supply (PSU) datasheet [31]. Fig. 10a shows the comparison between experimental and simulation results of THD% vs. modulation index for each case analyzed at no load conditions. Moreover, the experimental values of THD% were evaluated for several values of the fundamental frequency. The experimental data confirmes the simulation results. In fact, the lowest THD% values were detected in the second case, where the 5th and 11th harmonics were eliminated. Moreover, as expected, no significant THD% variations were detected as the fundamental frequency varies. Proposed approach is suitable in several applications where different fundamental working frequencies are required. In order to demonstrate the improved performance of the proposed algorithm with respect to other traditional SHE algorithms, the experimental THD% values were compared with those obtained by using the SHE algorithm discussed in [8]. In detail, Fig. 10b shows that the proposed approach reduces THD% in almost the whole modulation range considered in Table I, with respect to the SHE algorithm proposed in [8] that individually eliminates the 5th, 7th, 11th and 13th harmonic, respectively. It is worth to notice that comparable results were detected only when modulation index was around 0.9. Therefore, it is possible to assert that lower values of the THD% were obtained with the proposed algorithm in all cases as shown in Fig. 10b.

B. Converter efficiency analysis

Efficiency is of paramount importance. This subsection aims to characterize the proposed algorithm in terms of converter efficiency for several values of the modulation index and the fundamental frequency. Moreover, it discusses the input power distribution provided by each DC source, that supplies each H-bridge module. The same working points, analyzed in the no-load tests, were considered for load tests by connecting an electric load with $R = 20\ \Omega$ and $L = 10$ mH. Fig. 11 shows the experimental converter efficiency vs. modulation index evaluated for different values of the fundamental frequency from 100 Hz to 400 Hz with 100 Hz steps.

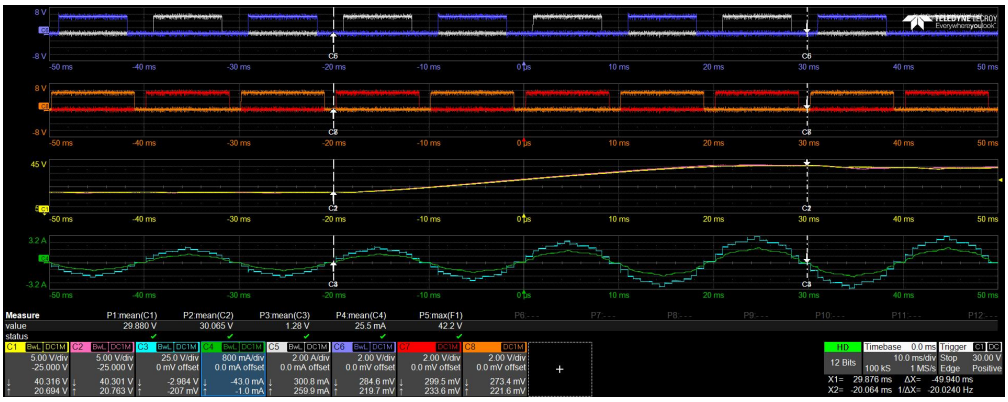

(a) SHE 5th and 13th with modulation index variation from m=0.34 to m=0.69.

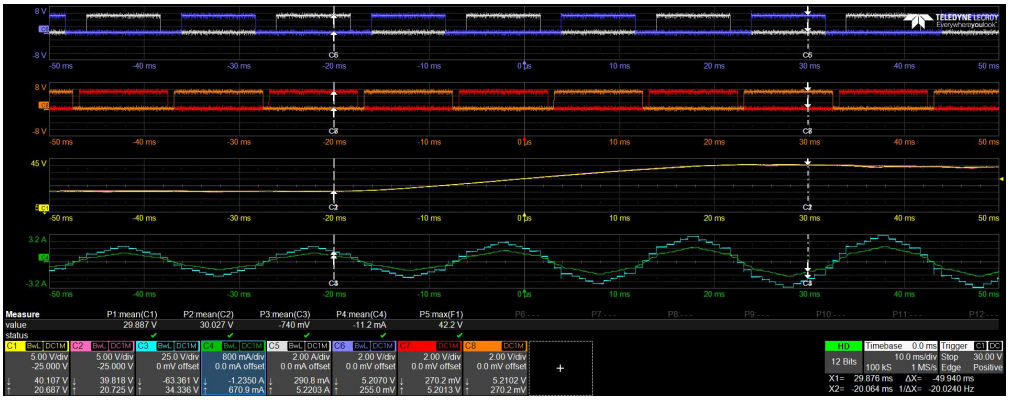

(b) SHE 7th and 13th with modulation index variation from m=0.35 to m=0.7.

Fig. 9. CHB inverter dynamic behaviour under DC voltage input change from 20 V to 40 V.

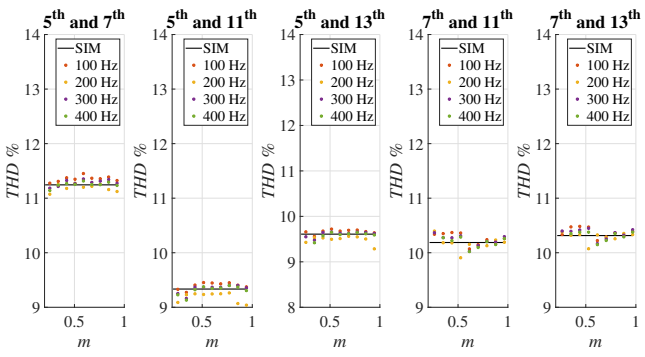

(a) Experimental vs. simulation results

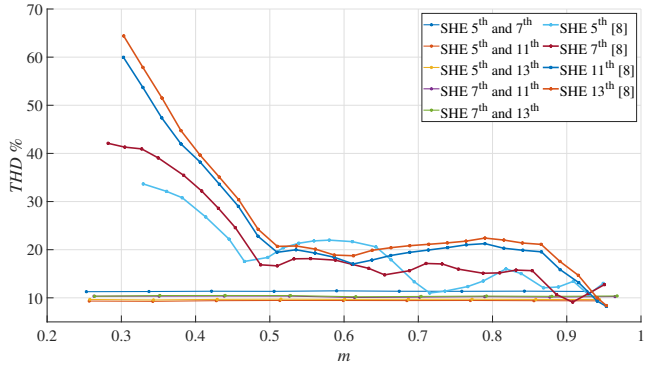

(b) Proposed algorithm vs. SHE in [8]

Fig. 10. Experimental comparison of THD% vs. modulation index among analyzed cases.

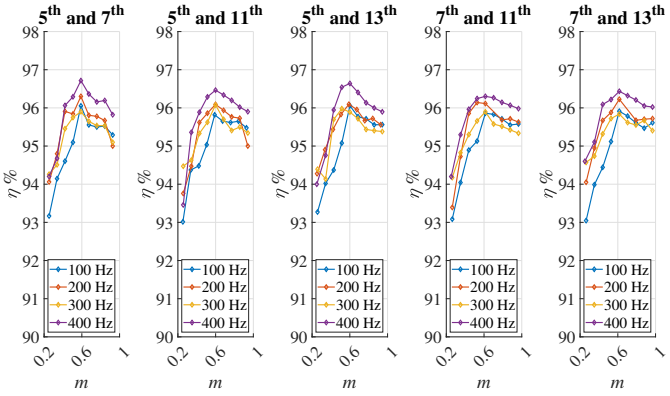

Fig. 11. Experimental converter efficiency vs. modulation index.

By varying the fundamental frequency, different load displacement power factor (DPF) values, 0.95, 0.85, 0.73 and 0.62 were obtained, respectively. The efficiency increases as the fundamental frequency increase. This phenomenon can be attributed to the RL load filter effect on the current harmonics. Fig. 12a shows converter efficiency vs. modulation index at 100 Hz (DPF=0.95) obtained with the proposed SHE approach, considering all cases in Table I , and obtained with traditional SHE proposed in [8] eliminating one by one the 5th, the 7th, the 11th and the 13th harmonic. Instead, Fig. 12b shows the same comparison of converter efficiency as in Fig.12a but at fundamental frequency equal to 400 Hz

(DPF=0.62), typical of avionics. It is worth to observe that, in all considered cases, converter efficiency is higher than with method [8], in particular at lower values of the modulation index, which means better control characteristics, especially for the 13$^{\text{th}}$ harmonic case and for all considered modulation index values.

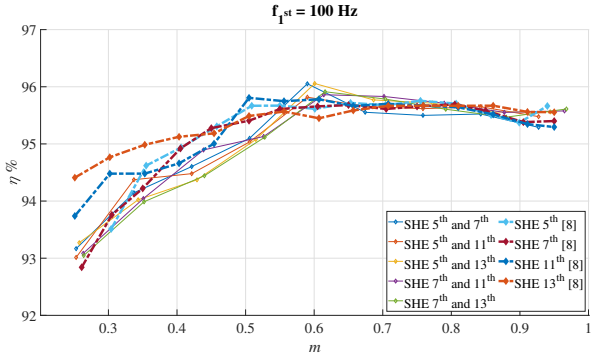

(a) 100 Hz

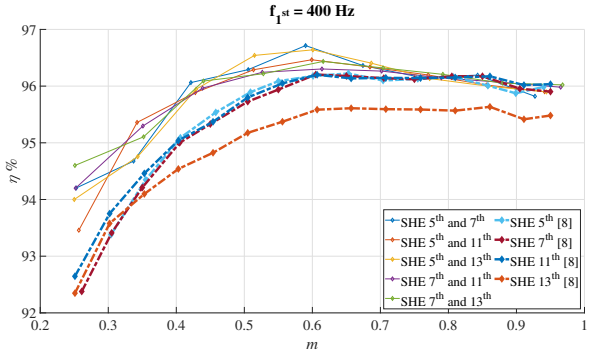

(b) 400 Hz

Fig. 12. Experimental converter efficiency vs. modulation index compared with respect to SHE algorithm in [8] at different fundamental frequency

Another interesting consideration is the DC power distribution between the H-Bridge modules $P_{\text{HB}i}$ as a function of the modulation index. Fig. 13 shows $P_{\text{HB}i}$ between two H-Bridge modules of the same phase, in percent with respect to the total input power $P_{\text{DC}j}$ $(j = A, B, C)$ of the same phase for the proposed approach (Fig.13a) and for SHE proposed in [8] (Fig.13b): the proposed algorithm returns an uniform DC power distribution, which is not the case of [8]. In summary, the analysis carried out and results obtained validate the effectiveness of the proposed SHE approach and highlight better performances with respect to the SHE approach proposed in [8].

VIII. Comparison with other SHE algorithms

In order to highlight the main benefits of the proposed SHE approach, a comparative analysis with other recent SHE approaches described in [29], [20], [13], and [21] has been carried out by considering as evaluation parameters the number and the order of eliminated harmonics, the implementation complexity, the capability to operate with continuity in a wide modulation index range, the computational cost and the solution employed. The results of such analysis are summarized in Table IV. Authors of [29] proposed a real-time solution for

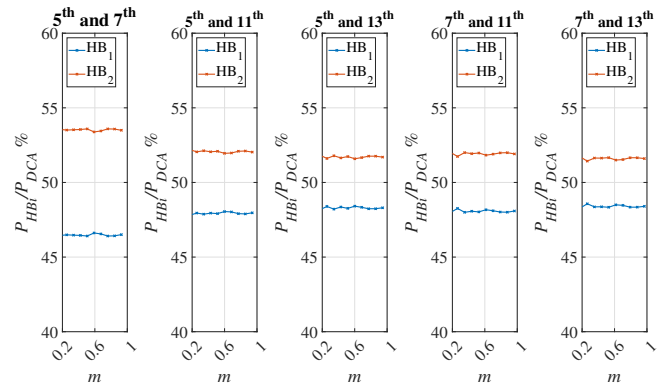

(a) Proposed algorithm

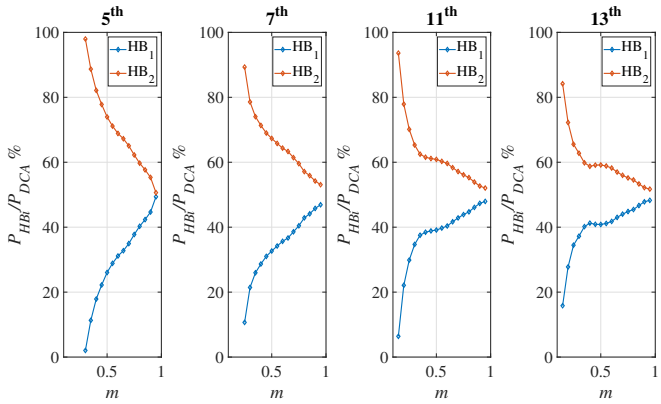

(b) SHE algorithm in [8]

Fig. 13. Experimental DC power distribution.

the determination of switching angles by using a proportional-integral (PI) controller which is based on the definition of an initial guess. The determination of the switching angles, that are suitable only for fundamental low-frequency applications, guarantees low-order harmonics elimination within the whole modulation index range and the elimination of $s-1$ harmonics. Nevertheless, this approach requires a significant amount of computational time and it does not consider high fundamental frequency analyses. Paper [20] proposed a SHE approach based on hybrid asynchronous particle swarm optimization Newton-Raphson (APSO) algorithm. According to authors, it provides efficient and accurate identification of the switching angles and fewer iterations than other genetic, Bee and PSO algorithms. However, although it requires just few iterations, its implementation is complex, the number of harmonics eliminated is equal to $s-1$ and it does not guarantee results for the whole modulation index range. Paper [13] proposed a hybrid artificial neural network-Newton Raphson (ANN-NR) based on a SHE procedure and suitable for CHB inverters for PV applications. Such an approach employs an ANN for the offline estimation of the switching angles that are used as initial guesses for the Newton-Raphson method. Since it requires just few iterations for optimal identification of the switching angles, it ensures quick convergence, however, it eliminates $s-1$ low-order harmonics but only within a modulation index range [0.68, 0.72]. Although authors estimate its power losses and efficiency, no comparative analysis

TABLE IV
COMPARISON OF THE PROPOSED SHE APPROACH WITH OTHER SHE APPROACHES.

Reference	Harmonics eliminated	Implementation complexity	Modulation index continuity variation	Computational cost	Solution
[8]	n	Low	Yes	Low	exact solution
[29]	$s-1$	High	Yes	High	approximate solution by NR
[20]	$s-1$	High	No	Low	approximate solution by APSO-NR
[13]	$s-1$	High	No	Low	approximate solution by AI
[21]	n and multiples	Low	Yes	Medium	exact solution
Proposed SHE	$n+1$ and multiples	Low	Yes	Low	exact solution

with other methods is reported. Finally, [21] proposed an interesting general mathematical solution for SHE purposes valid for both symmetrical and asymmetrical CHB inverter configurations. The approach eliminates the targeted harmonics in a wide range of modulation index and, in asymmetrical CHB configurations, guarantees the cancellation of a larger number of harmonics, but at the cost of higher implementation complexity. Its computation cost increases with the number of eliminated harmonics, and its THD is a function of the modulation index value. For symmetrical multilevel inverter configurations, eliminated harmonics are equal to n and multiples. It is worth noticing that all previously considered papers do not include either a detailed efficiency analysis or the DC power distribution among the H-Bridge modules as well.

To compare THD, the methods proposed in [32] and in [10] were implemented and analyzed. The first method, the so-called middle-level SHE pulse amplitude modulation (ML-SHE-PAM), does not delete the harmonics having order $2(l-1)z \pm 1$, the second one, the SHE pulse amplitude width modulation (SHE-PAWM), does not delete the harmonics having order $2lz \pm 1$ with $z = 1, 2, ...$ Fig 14 shows a comparison among the phase voltage THD% obtained with the proposed approach and ML-SHE-PAM and SHE-PAWM approaches considering up to 301^{th} harmonic. The proposed method offers better performances with CHB inverters with few levels, whereas, its performances are comparable in the case of thirty-three-level CHB inverters. Hence, the proposed method outperforms the other methods in cases of more practical interest.

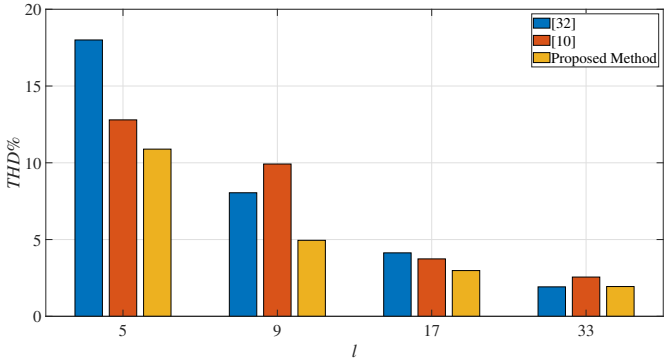

Fig. 14. Comparison among phase voltage THD% obtained with the proposed approach and the considered ML-SHE-PAM and SHE-PAWM approaches.

IX. CONCLUSIONS

In this paper, a new selective harmonics elimination algorithm based on a recursive application of the Prosthaphaeresis formulas has been proposed for the elimination of $n+1$ harmonics and their multiples from the output voltage waveform of an l-level CHB inverter with s equal DC sources $V(m)$. Proposed approach has been numerically evaluated for different CHB inverter configurations and experimentally validated with a three-phase five-level CHB inverter. Several tests with or without load and considering several case studies confirm that the proposed approach is very effective. Comparisons with the modulation described in [8] highlight much improved performance and lower computational effort. Overall efficiency improves increasing frequency, which makes it suitable for variable speed electrical drives. Moreover, a comparison with som recent SHE approaches described in the literature is reported to highlight the main benefits of the proposed approach. The algorithm can be usesul in multilevel photovoltaic inverters, too, taking benefit from DC-DC stages used in maximum power point tracking.

ACKNOWLEDGMENT

This work was financially supported by MUR-PRIN 2017, Project 2017MS9F49, by Sustainable Development and Energy Saving Laboratory (SDESLAB), Laboratory of Electrical Applications (LEAP), Electrical Drive Applications Laboratory (EDALAB) of the Department of Engineering of University of Palermo, Italy, and by DigiPower srl, 67100 L'Aquila, Italy.

REFERENCES

[1] M. S. A. G. Konstantinou, and V. G. Agelidis, "A review of multilevel selective harmonic elimination PWM: formulations, solving algorithms, implementation and applications," *IEEE Trans. Pow. Electron.*, vol. 30, no. 8, pp. 4091–4106, Aug. 2015.

[2] M. Trabelsi, H. Vahedi and H. Abu-Rub, "Review on Single-DC-Source Multilevel Inverters: Topologies, Challenges, Industrial Applications, and Recommendations," in IEEE Open Journal of the Industrial Electronics Society, vol. 2, pp. 112-127, 2021.

[3] A. I. Elsanabary, G. Konstantinou, S. Mekhilef, C. D. Townsend, M. Seyedmahmoudian and A. Stojcevski, "Medium Voltage Large-Scale Grid-Connected Photovoltaic Systems Using Cascaded H-Bridge and Modular Multilevel Converters: A Review," in IEEE Access, vol. 8, pp. 223686-223699, 2020.

[4] S. S. Lee, B. Chu, N. R. N. Idris, H. H. Goh, and Y. E. Heng, "Switched-battery boost-multilevel inverter with GA optimized SHEPWM for standalone application," *IEEE Trans. Ind. Electron.,* vol. 63, no. 4, pp. 2133–2142, Apr. 2016.

[5] J. He, Q. Li, C. Zhang, J. Han, C. Wang, "Quasi-Selective Harmonic Elimination (Q-SHE) Modulation-Based DC Current Balancing Method for Parallel Current Source Converters," *IEEE Trans. Pow. Electron.*, vol. 34, no. 8, pp. 8201–8212, Aug. 2019.

[6] H. Zhao, S. Wang, A. Moeini, "Critical Parameter Design for a Cascaded H-Bridge With Selective Harmonic Elimination/Compensation Based on Harmonic Envelope Analysis for Single-Phase Systems," *IEEE Trans. Ind. Electron.*, vol. 66, no. 4, pp. 2914–2925, Apr. 2019.

[7] C. Buccella, C. Cecati, M. G. Cimoroni, K. Razi, "Analytical method for pattern generation in five-level cascaded H-bridge inverter using selective harmonic elimination," *IEEE Trans. Ind. Electron.,* vol. 61, no. 11, pp. 5811-5819, Nov. 2014.

[8] C. Buccella, C. Cecati, M. G. Cimoroni, G. Kulothungan, A. Edpuganti, A. Kumar Rathore, "A Selective Harmonic Elimination Method for Five-Level Converters for Distributed Generation," *IEEE Journal of Emerg. and Select. topic in Pow. Elec.,* vol. 5, no. 2, pp. 775 - 783, June 2017.

[9] G. Schettino, F. Viola, A. O. Di Tommaso, P. Livreri and R. Miceli, "Experimental Validation of a Novel Method for Harmonic Mitigation for a Three-Phase Five-Level Cascaded H-Bridges Inverter," *IEEE Trans. Ind. Applicat.*, vol. 55, no. 6, pp. 6089-6101, Nov.-Dec. 2019.

[10] C. Buccella, M.G. Cimoroni, M. Tinari, C. Cecati, "A new pulse active width modulation for multilevel converters," *IEEE Trans. Pow. Electron.*, vol. 34, no. 8, pp. 7221-7229, Aug. 2019.

[11] R. Sajadi, H. Iman-Eini, M. K. Bakhshizadeh, Y. Neyshabouri and S. Farhangi, "Selective Harmonic Elimination Technique With Control of Capacitive DC-Link Voltages in an Asymmetric Cascaded H-Bridge Inverter for STATCOM Application," *IEEE Trans. Ind. Electron.*, vol. 65, no. 11, pp. 8788-8796, Nov. 2018.

[12] L. K. Haw, M. S. A. Dahidah and H. A. F. Almurib, "SHE–PWM Cascaded Multilevel Inverter With Adjustable DC Voltage Levels Control for STATCOM Applications," *IEEE Trans. Pow. Electron.*, vol. 29, no. 12, pp. 6433-6444, Dec. 2014.

[13] S. Padmanaban, C. Dhanamjayulu and B. Khan, "Artificial Neural Network and Newton Raphson (ANN-NR) Algorithm Based Selective Harmonic Elimination in Cascaded Multilevel Inverter for PV Applications," *IEEE Access*, vol. 9, pp. 75058-75070, 2021.

[14] A. Poorfakhraei, M. Narimani and A. Emadi, "A Review of Modulation and Control Techniques for Multilevel Inverters in Traction Applications," *IEEE Access*, vol. 9, pp. 24187-24204, 2021.

[15] Z. Ni, A. H. Abuelnaga and M. Narimani, "A New Fault-Tolerant Technique Based on Nonsymmetrical Selective Harmonic Elimination for Cascaded H-Bridge Motor Drives," *IEEE Trans. Ind. Electron.*, vol. 68, no. 6, pp. 4610-4622, June 2021.

[16] M. Steczek, P. Chudzik and A. Szeląg, "Combination of SHE- and SHM-PWM Techniques for VSI DC-Link Current Harmonics Control in Railway Applications," *IEEE Trans. Ind. Electron.*, vol. 64, no. 10, pp. 7666-7678, Oct. 2017.

[17] G. Schettino, C. Nevoloso, R. Miceli, A. O. D. Tommaso and F. Viola, "Impact Evaluation of Innovative Selective Harmonic Mitigation Algorithm for Cascaded H-Bridge Inverter on IPMSM Drive Application," *IEEE Open Journal of Ind. Applicat.,* vol. 2, pp. 347-365, 2021.

[18] W. M. Fei, Y. L. Zhang, and X. B. Ruan, "Solving the SHEPWM nonlinear equations for three-level voltage inverter based on computed initial values," *IEEE Appl. Power Electron. Conf.,* pp. 1084–1088, Feb. 2007.

[19] K. Haghdar, "Optimal DC Source Influence on Selective Harmonic Elimination in Multilevel Inverters Using Teaching–Learning-Based Optimization," *IEEE Trans. Ind. Electron.*, vol. 67, no. 2, pp. 942–949, Feb. 2020.

[20] M. A. Memon, S. Mekhilef, and M. Mubin, "Selective harmonic elimination in multilevel inverter using hybrid APSO algorithm," *IET Pow. Electron.*, vol. 11, no. 10, pp. 1673–1680, 2018.

[21] M. Ahmed et al., "General Mathematical Solution for Selective Harmonic Elimination," *IEEE Journal of Emerg. and Select. topic in Pow. Elec.,* vol. 8, no. 4, pp. 4440-4456, Dec. 2020.

[22] K. Yang et al., "Unified Selective Harmonic Elimination for Multilevel Converters," *IEEE Trans. Pow. Electron.*, vol. 32, no. 2, pp. 1579-1590, Feb. 2017.

[23] A. Routray, R. Kumar Singh, R. Mahanty, "Harmonic Minimization in Three-Phase Hybrid Cascaded Multilevel Inverter Using Modified Particle Swarm Optimization," *IEEE Trans. Ind. Inf.*, vol. 15, no. 8, pp. 4407-4417, Aug. 2019.

[24] A. Kavousi, B. Vahidi, R. Salehi, M. Bakhshizadeh, N. Farokhnia, and S. S. Fathi, "Application of the bee algorithm for selective harmonic elimination strategy in multilevel inverters," *IEEE Trans. Pow. Electron.*, vol. 27, no. 4, pp. 1689–1696, Apr. 2012.

[25] F. Filho, H. Z. Maia, T. H. A. Mateus, B. Ozpineci, L. M. Tolbert, and J. O. P. Pinto, "Adaptive selective harmonic minimization based on ANNs for cascade multilevel inverters with varying DC sources," *IEEE Trans. Ind. Electron.,* vol. 60, no. 5, pp. 1955–1962, Mar. 2013.

[26] K. Yang, Z. Yuan, R. Yuan, W. Yu, J. Yuan and J. Wang, "A Groebner Bases Theory-Based Method for Selective Harmonic Elimination," *IEEE Trans. Pow. Electron.*, vol. 30, no. 12, pp. 6581-6592, Dec. 2015.

[27] H. Zhao, T. Jin, S. Wang and L. Sun, "A Real-Time Selective Harmonic Elimination Based on a Transient-Free Inner Closed-Loop Control for Cascaded Multilevel Inverters," *IEEE Trans. Pow. Electron.*, vol. 31, no. 2, pp. 1000-1014, Feb. 2016, doi: 10.1109/TPEL.2015.2413898.

[28] K. Yang, M. Feng, Y, Wang, X, Lan, J, Wang, D. Zhu, W. Yu, "Real-Time Switching Angle Computation for Selective Harmonic Control," *IEEE Trans. Pow. Electron.*, vol. 34, no. 8, pp. 8201–8212, Aug. 2019.

[29] M. Ahmed, A. Sheir, and M. Orabi, "Real-Time Solution and Implementation of Selective Harmonic Elimination of Seven-Level Multilevel Inverter," *IEEE Journal of Emerg. and Select. topic in Pow. Elec.,* vol. 5, no. 4, pp. 1700 - 1709, Dec. 2017.

[30] M. H. Etesami, D. M. Vilathgamuwa, N. Ghasemi, D. P. Jovanovic, "Enhanced metaheuristic methods for selective harmonic elimination technique," *IEEE Trans. on Ind. Inf.*, vol. 14, no. 12, pp. 5210–5220, Dec. 2018.

[31] https://www.meanwell.com/Upload/PDF/RSP-2400/RSP-2400-SPEC.PDF.

[32] P. L. Kamani and M. A. Mulla, "Middle-Level SHE Pulse-Amplitude Modulation for Cascaded Multilevel Inverters," in *IEEE Transactions on Industrial Electronics*, vol. 65, no. 3, pp. 2828-2833, March 2018.